Stability of locking in mutually delay-coupled semiconductor lasers

H. Erzgräber[a], D. Lenstra[a,b], and B. Krauskopf[c,a]

[a]Natuurkunde en Sterrenkunde, Vrije Universiteit Amsterdam, The Netherlands
[b]COBRA Research Institute, Technische Universiteit Eindhoven, The Netherlands
[c]Department of Engineering Mathematics, University of Bristol, UK

ABSTRACT

We investigate the continuous wave solutions of a system of two mutually delay coupled semiconductor lasers. These continuous wave solutions, which we refer to as compound laser modes (CLMs), are locked solutions of the coupled laser system where both lasers lase at a common frequency. We model the system by a set of delay differential rate equations, where we assume that, apart from a possible detuning in their free running optical frequencies, the lasers are identical. We show how the structure and the stability of the CLMs depend on the main parameters, namely, the feedback phase, the feedback rate, the pump parameter, and the detuning.

We identify two mechanisms for creating CLMs. First, CLMs emerge from the off-state of the coupled laser system in Hopf bifurcations. Second, CLMs are created in pairs in saddle-node bifurcations. For the special case of zero detuning we also find pitchfork bifurcations that organize the CLM structure. We show in which parameter regions CLMs exist, where they are stable, and which bifurcation curves form the boundary of the stable locking region.

Keywords: semiconductor laser, mutual coupling, delay, bifurcation analysis, compound laser modes

1. INTRODUCTION

Two coupled oscillators are locked if they operate with a common frequency, even though their natural solitary frequencies are different. A prominent example is the Adler locking scenario of two instantaneously coupled oscillators.[1] We are interested here in the influence that delay in the coupling may have on the possibility of locking or synchronization, which is of fundamental interest in physics and still only partially understood; see, *e.g.*, Ref. [2, 3]. Coupled semiconductor lasers are a prototype example of two coupled oscillators[4] and, as such, very interesting systems for studying nonlinear dynamics of coupled oscilators. Semiconductor laser show a great dynamical variety, and the agreement between experiment and theory is very good; see, *e.g.*, Refs. [4–9]. Moreover, coupled lasers are also of great technological interest because of possible application, such as bistable devices for optical flip-flops, high-frequency generation for optical clocks, or secure communication with a chaotic carrier; see, *e.g.*, Refs. [5, 10–12]. It is known that even weak coupling between different optical components can lead to complicated dynamics.[13]

In this paper we show how the structure and the stability of the compound laser modes change as the main parameters are changed. We consider here the influence of the feedback phase, the feedback rate, the pump parameter, and the detuning between the lasers. All these parameters vitally influence the CLM structure, which is of great importance for understanding more complicate dynamics of coupled laser system. CLMs can actually be created in two different ways: they can emerge from the off-state of the coupled laser system in Hopf bifurcations (the first of which corrsponds to the threshold of the coupled laser system), and they can appear in pairs in saddle-node bifurcations. We use bifurcation analysis with DDE-BIFTOOL [14] to study in which parameter regions CLMs are stable and which type of instabilities is encountered at the boundary of the locking region. In our investigations the case of zero detuning plays the role of an organising center, as it features pitchfork bifurcations due to the additional phase space symmetry of exchanging the two lasers.

Further author information: (Send correspondence to H. Erzgräber)
H. Erzgräber: E-mail: h.erzgraber@few.vu.nl

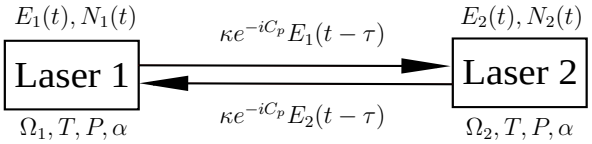

Figure 1. Sketch of the delay-coupled laser system.

This paper is structured as followed. First, we introduce the system and the model equations in Sec. 2. In Sec. 3 we discuss different types of CLMs in the commonly used representation of frequency versus inversion for fixed pump parameter and coupling rate, and for zero and non-zero detuning. In Sec. 4 we show how the number of CLMs and, therefore, the complexity of the coupled laser system, increases as the coupling rate is increased symmetrically for both lasers. Section 5 discusses the influence of the pump parameter on the locking regions for changing detunings and a fixed coupling rate. We end with conclusions in Sec. 6.

2. THE COUPLED LASER SYSTEM

The two lasers are coherently coupled via there optical fields, *i.e.*, a fraction κ of the light emitted by laser 1 is injected into laser 2, and vice versa. Apart from a difference in their free running optical frequencies we assume two identical laser and symmetrical coupling conditions; Fig. 1 shows a sketch. The lasers are spatially separated, which results in a delay of $\tau = \frac{l}{c}$, where l is the distance between the lasers a c the speed of light. Furthermore, while traveling from one laser to the other, the optical fields accumulate the coupling phase C_p. This delay-coupled system can be described well by a set of delay differential equations:

$$\frac{dE_1(t)}{dt} = (1+i\alpha)N_1(t)E_1(t) + \kappa e^{-iC_p}E_2(t-\tau) - i\Delta E_1(t)\,, \tag{1}$$

$$\frac{dE_2(t)}{dt} = (1+i\alpha)N_2(t)E_2(t) + \kappa e^{-iC_p}E_1(t-\tau) + i\Delta E_2(t)\,, \tag{2}$$

$$T\frac{dN_1(t)}{dt} = P - N_1(t) - (1+2N_1(t))|E_1(t)|^2\,, \tag{3}$$

$$T\frac{dN_2(t)}{dt} = P - N_2(t) - (1+2N_2(t))|E_2(t)|^2\,. \tag{4}$$

Here the indices 1 and 2 distinguish the equations for the two laser; see also Ref. [15]. In these equations the time t is rescaled with the photon life time (which is typically of the order of 10 ps). $N_{1,2}(t)$ are the inversions of laser 1 and laser 2 with respect to the inversion at threshold. $E_{1,2}(t)$ are the envelopes of the complex optical field $\mathcal{E}_{1,2}(t) = E_{1,2}(t)e^{i\Omega t}$, with the mean optical frequency $\Omega = (\Omega_1 + \Omega_2)/2$. The parameters $\Omega_{1,2}$ are the solitary

Table 1. The parameters and their values.

symbol	laser parameter	value
α	linewidth enhancement factor	2.5
T	electron life time	392.0
τ	coupling time	20.0
C_p	coupling phase	$[-\pi, \pi]$
Δ	detuning	$[-0.1, 0.1]$
κ	coupling strength	$[0, 0.2]$
P	pump parameter	selected values in $[-0.093, 0.3]$

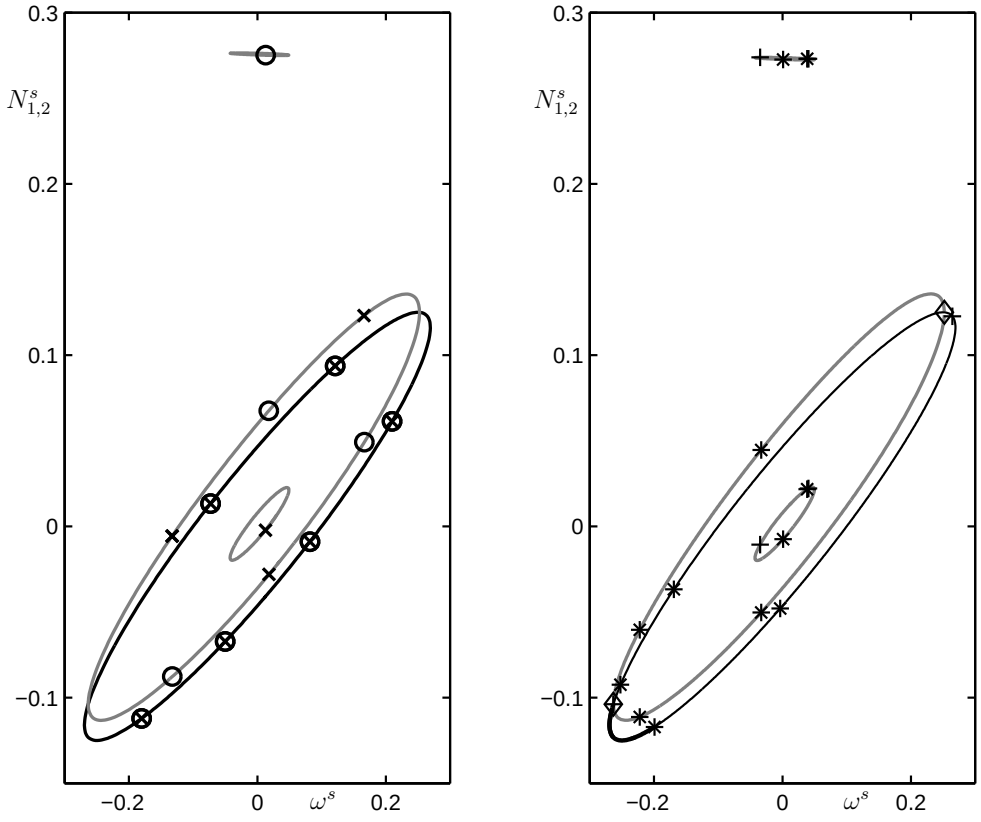

Figure 2. The different CLMs for zero detuning, $\Delta = 0$, in the $(\omega^s, N^s_{1,2})$-projection. Black indicates constant-phase CLMs and gray variable-phase CLMs. In panel (a) the circles ($\circ$) and the crosses ($\times$) denote the inversions of laser 1 and laser 2, respectively. In panel (b) pluses ($+$) denote saddle-node bifurcations, diamonds ($\diamond$) pitchfork bifurcations and stars ($*$) Hopf bifurcations; thick curves indicate stable CLMs; $P = 0.3$ and $\kappa = 0.1$.

lasers frequencies of laser 1 and laser 2, respectively. The parameter Δ describes the detuning between these two solitary lasers frequencies, and C_p is the coupling phase that the optical fields accumulate while traveling from one laser to the other, namely,

$$\Delta = \frac{\Omega_2 - \Omega_1}{2}\,, \quad C_p = \frac{\Omega_1 + \Omega_2}{2}\tau = \Omega\tau\,. \tag{5}$$

Alternatively, the solitary lasers frequencies $\Omega_{1,2}$ can be expressed in terms of the detuning Δ and the coupling phase C_p as

$$\Omega_1 = \frac{C_p}{\tau} - \Delta\,, \quad \Omega_2 = \frac{C_p}{\tau} + \Delta\,. \tag{6}$$

The remaining parameters are the linewidth enhancement factor α, the electron life time T, the coupling rate κ, and the pump parameter P. The values of all parameters can be found in Table 1.

3. THE COMPOUND LASER MODES

The CLMs are the basic solutions of equations (1)–(4), and they can be written in the form

$$E_1(t) = R^s_1 e^{i\omega^s t}\,, \quad E_2(t) = R^s_2 e^{i\omega^s t + i\sigma}\,, \quad N_1(t) = N^s_1\,, \quad N_2(t) = N^s_2\,, \tag{7}$$

where $R^s_{1,2}, N^s_{1,2}, \omega^s$ and σ are real valued. In this ansatz $R^s_{1,2}$ are the positive amplitudes of the optical fields and $N^s_{1,2}$ the inversions of laser 1 and 2, respectively. Further, ω^s is the lasers's common optical frequency with respect to the mean frequency Ω, and σ is a possible time-independent phase shift.

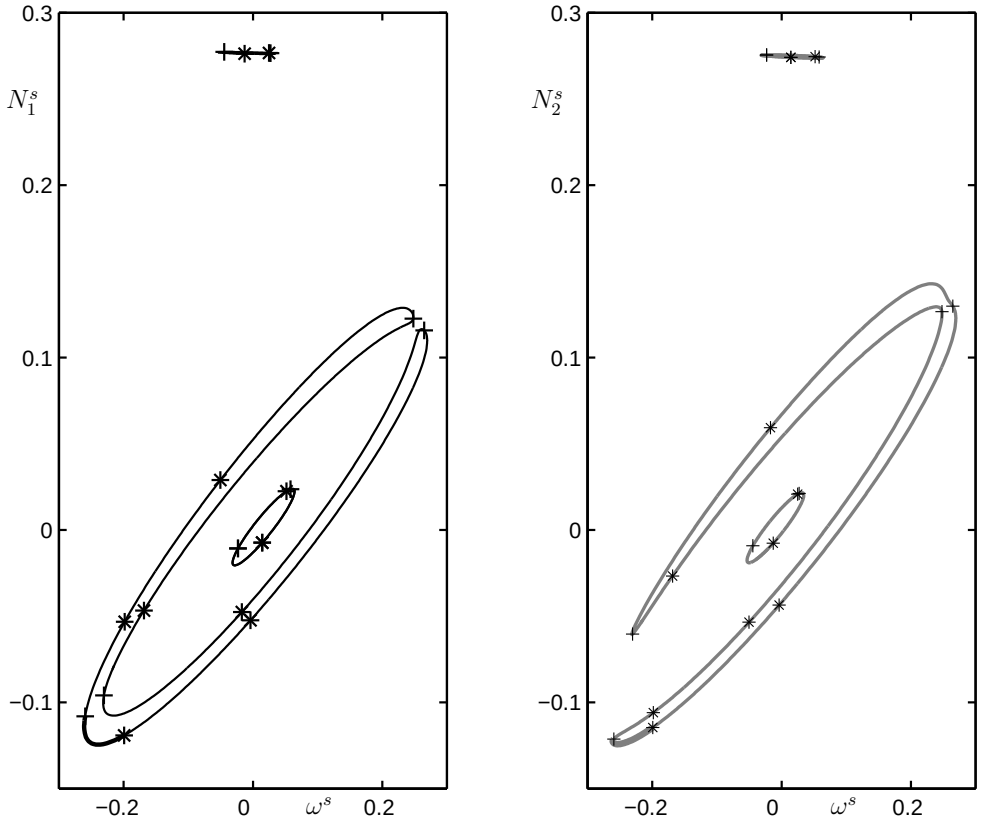

Figure 3. The different CLMs for non-zero detuning, $\Delta = 0.01$, in the (ω^s, N_1^s)-projection for laser 1 (a), and in the (ω^s, N_2^s)-projection for laser 2 (b). Pluses (+) denote saddle-node bifurcations and stars (∗) Hopf bifurcations; thick curves indicate stable CLMs; $P = 0.3$ and $\kappa = 0.1$.

Figure 2 depicts the CLMs for zero detuning, $\Delta = 0$, in the $(\omega^s, N_{1,2}^s)$-projection for a pumping of $P = 0.3$ well above threshold and the intermediate level of coupling of $\kappa = 0.01$. For a fixed value of the coupling phase C_p a finite number of CLMs exist. In Fig. 2(a) they are plotted as circles (∘) for the inversion of laser 1 and crosses (×) for the inversion of laser 2. The closed ellipse-like curves are traced out by the respective CLM as the coupling phase C_p is changed over one interval of 2π; see Ref. [16]. In particular, two types of CLMs exist. There are CLMs for which the inversions of both lasers are identical, and they trace out the black ellipse. Furthermore, there are CLMs for which the inversions of the two lasers are *not* identical, and they trace out the gray ellipses. Note that the inversion of the laser 1 lies on the lower curve and the inversion of the laser 2 on the upper curve, and vice verse. These two types of solutions are possible because of the symmetries of Eq. (1)–(4). For $\Delta = 0$ there is an additional reflectional symmetry, so that every CLM comes in two identical pairs or has a symmetric counterpart.[16] The CLMs that come in identical pairs are called *constant-phase CLMs*, because the phase σ is a constant (as a function of C_p) and can only take the values $\sigma = 0$ or $\sigma = \pi$. Note that for constant-phase CLMs the inversions of both lasers are identical, that is, $N_1^s = N_2^s$. The CLMs that come in symmetric pairs are called *variable-phase CLMs*, because the phase σ is a function of C_p (and, hence, of the frequency ω^s). For variable-phase CLMs the inversions of both lasers are *not* identical, that is, $N_1^s \neq N_2^s$.

Figure 2(b) shows the stability information for the different branches of CLMs in Fig. 2(a). Stable parts are plotted as thick curves; notice that only the low-inversion part of the constant-phase curve is stable. When C_p is changed and a CLM enters this thick plotted part of the curve then this CLM is stable. The stability region is bounded by a saddle-node bifurcation (+) to the right and by a Hopf bifurcation (∗) to the left. Moreover, the constant-phase CLMs can undergo additional bifurcations as C_p is changed. Apart from additional Hopf

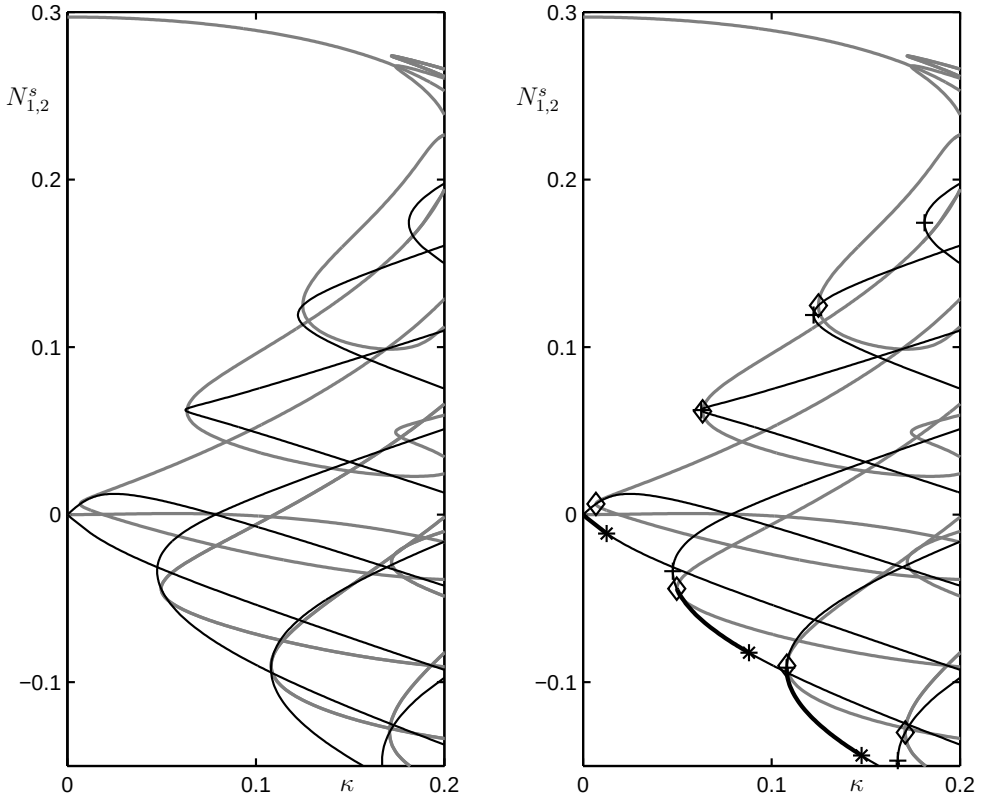

Figure 4. One-parameter bifurcation diagram of the CLMs for zero detuning, $\Delta = 0$, in the $(\kappa, N^s_{1,2})$-projection. The constant-phase CLMs are plotted in black and the variable-phase CLMs in gray; panel (a) shows the CLMs for $\kappa = 0.1$ and panel (b) shows bifurcations points; namely, pluses (+) denote saddle-node bifurcations, diamonds ($\diamond$) pitchfork bifurcations and stars ($*$) Hopf bifurcations; thick curves indicate stable CLMs; $P = 0.3$ and $C_p = 0.0$.

bifurcations there are two pitchfork bifurcations ($\diamond$). In these pitchfork bifurcations variable phase CLMs are born and destroyed. The second set of variable CLMs — on the small ellipses around the $(\omega^s, N^s_{1,2} \approx (0, 0))$ and $(\omega^s, N^s_{1,2} \approx (0, 0.27))$ — are created and lost in separate saddle-node bifurcations.

Figure 3 shows what the CLM structure looks like for a non-zero detuning of $\Delta = 0.01$ and the same values of $P = 0.3$ and $\kappa = 0.1$. To distingush between the two lasers, the (ω^s, N^s_1)-projection for laser 1 is shown in panel (a) and the (ω^s, N^s_2)-projection for laser s is shown in panel (b). As a result of the non-zero detuning the two pitchfork bifurcations unfold to saddle-node bifurcations.[16] In the $(\omega^s, N^s_{1,2})$-projections a horseshoe-like structure is formed for both lasers. For laser 1 the horseshoe is open at the high-inversion part and for laser 2 the horseshoe is open in the low-inversion part. Note that a CLM for fixed C_p corresponds to a point in panel (a) and one in panel (b) with the same frequency ω^s. Stable CLMs can be found on a small part in the lowinversion region of the horseshoes. This stable locking region is bounded by a saddle-node bifurcation to the left and by a Hopf bifurcation to the right. In addition the CLMs on the small ellipses around $(\omega^s, N^s_{1,2} \approx (0, 0))$ and $(\omega^s, N^s_{1,2} \approx (0, 0.27))$ split up into two pairs, which are slightly shifted with respect to each other.

4. CLM DEPENDENCE ON THE COUPLING RATE

In this section we show how CLMs are created as the coupling strength κ is increased symmetrically for both lasers. Figure 4 shows the $(\kappa, N^s_{1,2})$-projection for $\Delta = 0$, where in black are plotted the constant-phase CLMs and in gray the variable-phase CLMs. In panel (a) only the structure of the CLMs is shown, while panel (b) displays the stability information and bifurcations. It can be seen that for $\kappa = 0$ there are in total four different

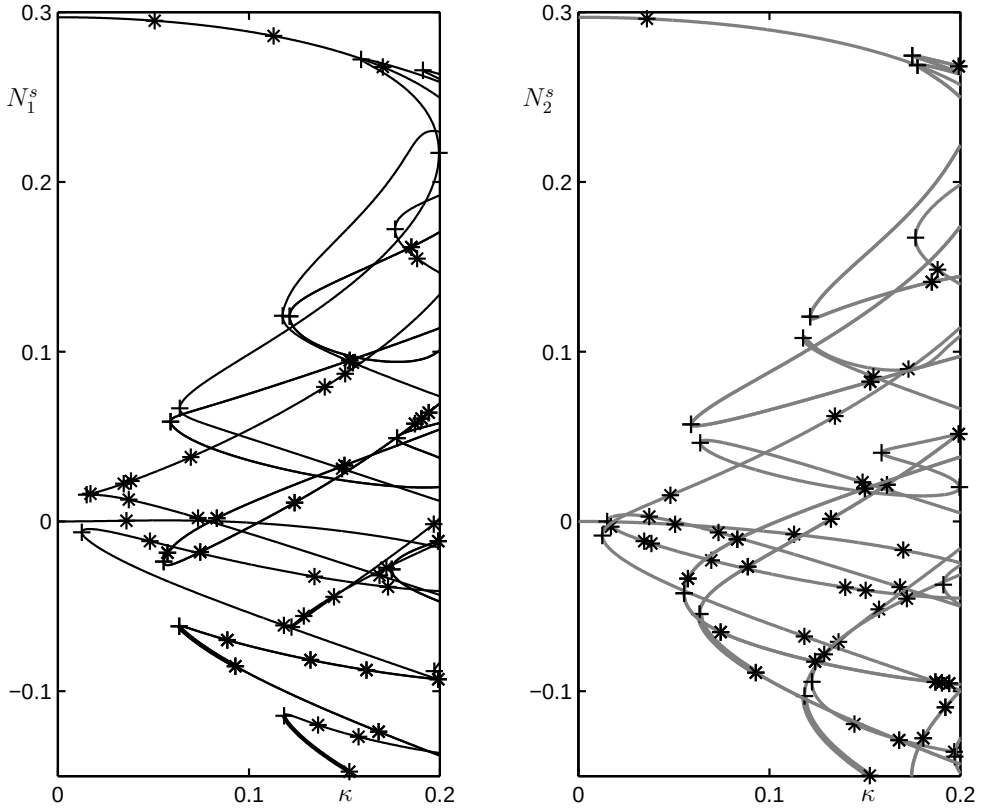

Figure 5. One-parameter bifurcation diagram of the CLMs for a non-zero detuning of $\Delta = 0.01$ in the (κ, N_1^s)-projection for laser 1 (a), and in the (κ, N_2^s)-projection for laser 2 (b). Pluses (+) denote saddle-node bifurcations and stars ($*$) Hopf bifurcations; thick curves indicate stable CLMs; $P = 0.3$ and $C_p = 0.0$.

CLMs. There are two constant-phase CLMs (in-phase and anti-phase CLMs), which emerge from the solitary laser solutions for which both lasers are in their on-state. These constant-phase CLMs are stable initially and then destabilize in a Hopf bifurcation ($*$). Furthermore, there are two variable-phase CLMs (recall that variable-phase CLMs come in symmetric pairs). They emerge from the solitary laser solution for which one laser is in its on-state and the other laser in its off-state, and vice versa. These variable-phase CLMs are unstable.

Additionly, as the coupling rate κ increases constant-phase CLMs are born in pairs in saddle-node bifurcations (+). One of these CLMs may initially be stable (in the low-inversion region) and then destabilizes in a Hopf bifurcation. Moreover, variable-phase CLMs are born in pairs in pitchfork bifurcations ($\diamond$) of constant-phase CLMs.

Again as the detuning Δ is 'switched on' all pitchfork bifurcations unfold to saddle-node bifurcations. This can be seen in Fig. 5 in the $(\kappa, N_{1,2}^s)$-projection for a non-zero detuning of $\Delta = 0.01$, where panel (a) shows the inversion of laser 1 in black and panel (b) the inversion of laser 2 in gray. Close to zero coupling ($\kappa = 0$) only those CLMs exist, which emerge from the solitary laser solution where laser 1 is off and laser 2 is on, and vice versa. As the coupling rate κ increases, additional CLMs are born in pairs in saddle-node bifurcations. Around $\kappa = 0$ no stable CLMs can be found, a minimum coupling strength is needed to enable stable locking; see the thick parts of the CLM branches.

5. CLM DEPENDENCE ON THE PUMP PARAMETER

A question of interest is how the stable locking region is influenced by changes of the pump parameter of the two lasers. In particular, the pump parameter influences the frequency of the lasers's internal relaxation oscillations. Therefore, complicated interactions between relaxation oscillations and, for example, oscillation on the scale of the coupling time of the lasers might be encountered.

In this section we discuss the shape of the stable locking region and the bifurcations at its boundary in the plane of detunings as the pump parameter is changed symmetrically for both lasers. Figure 6 shows the (Ω_1, Ω_2)-projection for different values of the pump parameter P. Note that this projection is equivalent to the (Δ, C_p)-projection used in Ref. [16, 17], according to transformation Eq. (6). However, from experimental point of view the (Ω_1, Ω_2)-projection is convenient, because typically one fixes the frequency of one laser and changes the frequency of the other laser.[9] Changing the frequency of both lasers by the same amount would than result in a change of the coupling phase C_p only, whereas changing the (solitary) frequencies of both lasers by the same magnitude but in opposite directions would result in a change of the detuning Δ only.

For very low pump parameter [Fig. 6(a)], just above the threshold of the coupled laser system, distinct regions of stable CLMs can be found. Indeed they are C_p copies of each other, *i.e*, from one region to the next C_p has increased by π. The CLMs are constant-phase CLMs and the boundary of the locking region is entirely formed by a Hopf bifurcation of the off-state of the coupled laser system (thin black curves). Because of the coupling the laser threshold is reduced and only for sufficiently small detuning the lasers can profit from the mutual coupling. When the detuning is too large then the effective coupling is too low and both lasers are off. As the pump parameter increases, the locking regions increase in size, so that adjacent C_p copies start to overlap each other. The points where they start to overlap give rise to additional bifurcations, namely Hopf bifurcation of CLMs (gray curves) and saddle-node bifurcations of CLMs (thick black curves). Because of the interactions of different CLMs, instabilities arise. This can be seen in Fig. 6(c), where small unstable islands separate adjacent stable locking regions. The boundary between the stable and unstable CLMs is initially formed by Hopf bifurcations of CLMs. As the pump parameter increases further, the unstable regions become larger and the boundary between the stable and unstable CLMs is formed by both Hopf bifurcations of CLMs and by bifurcations of CLMs [Fig. 6(e)]. Eventually, for sufficiently high pumping, a typical triangular locking region can be found [Fig. 6(h)], which qualitatively does not change anymore for an even higher pump parameter. Now the whole detuning plane is filled with either stable or unstable CLMs.

Note that most of the qualitative changes occur for negative P, *i.e.*, below the threshold of the solitary lasers. It clearly depends quite sesitively on the value of the pump parameter which curves bound the locking region, namely via a Hopf bifurcation of the off-state, via Hopf of a CLM or via asaddle-node bifurcation of CLMs. Each of these possibilities leads to qualitatively different dynamics, which are beyond the sope of this paper.

6. CONCLUSIONS

In conclusion we discussed the compound laser modes of two mutually delay-coupled semiconductor laser as a function of the main parameters, namely the feedback phase, the feedback rate, the pump parameter and the detuning. CLMs are locked solutions where both lasers operate at the same frequency, but with possibly different intensities. We found that the CLMs may be stable even though the lasers are detuned. Two mechanisms can create CLMs. One is by a Hopf bifurcation of the off-state, which is typical when the pump parameter is changed. The other is by saddle-node bifurcations of CLMs, which is typical when the feedback phase, the feedback rate, or the detuning are changed.

Knowledge of the CLM structure — and this includes the unstable CLMs as well — is the key to understanding the dynamics of delay-coupled lasers. The geometric picture we provided here paves the way for future studies of more complicated dynamics of coupled laser systems.

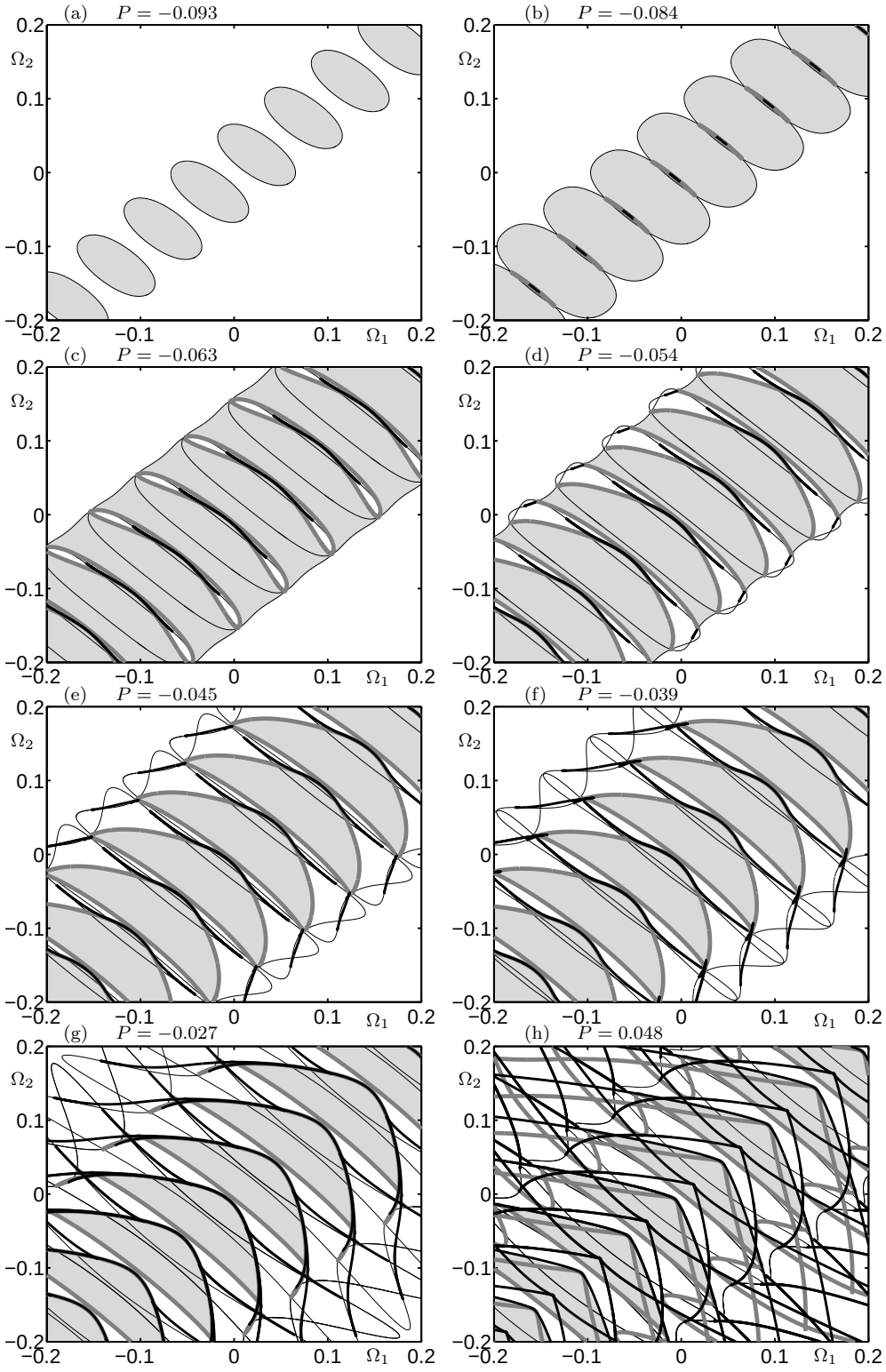

Figure 6. Two-parameter bifurcation diagrams of the CLMs for $\kappa = 0.1$ in the (Ω_1, Ω_2)-projection for different values of the pump parameter as indicated in the panels. In the gray areas CLMs are stable, thin black curves are Hopf bifurcations of the off-state, thick black curves are saddle-node bifurcations of CLMs, and gray curvess are Hopf bifurcations of CLMs.

REFERENCES

1. R. Adler, "A study of locking phenomena in oscillators," *Proc. IRE* **34**, pp. 351–357, 1946. neu abgedruckt in *Proc. IEEE 61*, (1973), 1380–1385.
2. G. Stepán, *Retarded Dynamical Systems: Stability and Characteristic Functions*, Longman Scientific and Technical, London, UK, 1989.
3. D. V. Ramana Reddy, A. Sen, and G. L. Johnston, "Time delay induced death in coupled limit cycle oscillators," *Phys. Rev. Lett.* **80**, pp. 5109–5112, 1998.
4. H.-J. Wünsche, S. Bauer, J. Kreissl, O. Ushakov, N. Korneyev, F. Henneberger, E. Wille, H. Erzgräber, M. Peil, W. Elsäßer, and I. Fischer, "Synchronization of delay-coupled oscillators: A study on semiconductor lasers," *Phys. Rev. Lett.* **94**, p. 163901, 2005.
5. I. Fischer, Y. Liu, and P. Davis, "Synchronization of chaotic semiconductor laser dynamics on subnanosecond time scales and its potential for chaos communication," *Phys. Rev. A* **62**, p. 011801, 2000.
6. T. Heil, I. Fischer, W. Elsäßer, J. Mulet, and C. R. Mirasso, "Chaos synchronization and spontaneous symmetry-breaking in symmetrically delay-coupled semiconductor lasers," *Phys. Rev. Lett.* **86**, pp. 795–798, 2001.
7. M. Peil, T. Heil, I. Fischer, and W. Elsäßer, "Synchronization of chaotic semiconductor laser systems: A vectorial coupling-dependent scenario," *Phys. Rev. Lett.* **88**, p. 174101, 2002.
8. J. Mulet, C. Mirasso, T. Heil, and I. Fischer, "Synchronization scenario of two distant mutually coupled semiconductor lasers," *J. Opt. B: Quantum Semiclass. Opt.* **6**, pp. 97–105, 2004.
9. H. Erzgräber, D. Lenstra, B. Krauskopf, E. Wille, M. Peil, I. Fischer, and W. Elsäßer, "Mutually delay-coupled semiconductor lasers: Mode bifurcation scenarios," *Opt. Commun.* **255(4-6)**, pp. 286–296, 2005.
10. M. T. Hill, H. de Waardt, and H. J. S. Dorren, "All-optical flip-flop based on coupled laser diodes," *IEEE J. Quantum Electron.* **QE-37**, pp. 405–413, 2001.
11. M. T. Hill, , H. J. S. Dorren, T. de Vries, X. J. M. Leijtens, J. H. den Besten, B. Smalbrugge, Y. Oei, H. Binsma, G. Khoe, and M. K. Smit, "A fast low-power optical memory based on coupled micro-ring lasers," *Nature* **432**, pp. 206–209, 2004.
12. M. Möhrle, B. Sartorius, C. Bornholdt, S. Bauer, O. Brox, A. Sigmund, R. Steingrüber, M. Radziunas, and H.-J. Wünsche, "Detuned grating multisection-RW-DFB lasers for high speed optical signal processing," *IEEE J. Select. Topics Quantum Electron.* **7**, pp. 217–223, 2001.
13. S. Wieczorek and W. W. Chow, "Chaos in practically isolated microcavity lasers," *Phys. Rev. Lett.* **92**, p. 213901, 2004.
14. K. Engelborghs, T. Luzyanina, and G. Samaey, "DDE-BIFTOOL v. 2.00 user manual: a matlab package for bifurcation analysis of delay differential equations.," Technical Report TW-330, Department of Computer Science, K. U. Leuven, Leuven, Oct. 2001.
15. J. Mulet, C. Masoller, and C. R. Mirasso, "Modeling bidirectionally coupled single-mode semiconductor lasers," *Phys. Rev. A* **65**, p. 063815, 2002.
16. H. Erzgräber, B. Krauskopf, and D. Lenstra, "Coupled laser modes of mutually delay-coupled lasers," *SIAM J. Appl. Dyn. Syst.* **5(1)**, pp. 30–65, 2006.
17. H. Erzgräber, B. Krauskopf, and D. Lenstra, "Mode structure of delay-coupled semiconductor lasers: influence of the pump current," *Journal of Optics B: Quantum and Semiclassical Optics* **7(11)**, pp. 361–371, 2005.